Derivation of the density of states of leaky photonic bands

Kazuo Ohtaka and Jun-ichi Inoue
Center for Frontier Science, Chiba University, 1-33 Yayoi-cho, Inage-ku, Chiba 263-8522, Japan

Syuuichi Yamaguti
Graduate School of Science and Technology, Chiba University, 1-33 Yayoi-cho, Inage-ku, Chiba 263-8522, Japan
(Received 26 November 2003; published 20 July 2004)

This paper presents the formula for the density of states (DOS) of photonic bands (PB's) in the leaky region of the phase space of a slab-type photonic crystal. It is expressed by the eigenphase shifts of the scattering matrix defined in terms of the complex transmission and reflection amplitudes of plane wave external incident light. The derivation is given for the general case in which a number of diffracted plane wave lights are produced by the incident lights. The DOS profile calculated as a function of frequency and wave vector enables us to obtain the dispersion relation and lifetime of leaky PB's. The usefulness of the derived formula is demonstrated by applying it to the PB structure of dielectric spheres, arrayed periodically to form a photonic crystal of finite thickness.

DOI: 10.1103/PhysRevB.70.035109 PACS number(s): 42.70.Qs

I. INTRODUCTION

Photonic crystals (PC's) are usually practically applied by preparing a system of finite thickness. When a photonic band (PB) mode is leaky, i.e., when its momentum and frequency lie within the light cone in phase space $(\mathbf{k},\omega)$, its finite lifetime decisively influences the capability of that mode in technological applications. Due to the lack of translational symmetry in a PC of finite thickness, the treatment of the lifetime caused by the leakage of PB modes through the PC surfaces is not at all straightforward. This is in clear contrast to an ideal PC of infinite size, where we can formulate a band-structure calculation as a standard eigenvalue problem of real eigenvalues.[1] In calculating the lifetime of a leaky PB mode, we must take account of its coupling with the plane wave states of the exterior region of a PC,[2,3] which by definition have a continuous spectrum of the density of states (DOS). For electrons, the finite lifetime of an electronic state resulting from its coupling with the other states of a continuous spectrum has been given much attention in the physics of metal, giving us some interesting topics, such as the Kondo effect and heavy fermions in Kondo lattices.[4] Although the basic mixing mechanisms of electrons and those of photons are conceptually very similar, one important point in the photonic problem in PC's is the need to obtain the lifetime and dispersion relation of PB's with a precision high enough to be integrated into a device design.

The purpose of the present paper is to present a method of calculating the DOS of leaky PB's of slab PC's, from which the dispersion and lifetime of PB's are both obtained precisely. The method is based on the calculation of a scattering matrix (S matrix) for a set of external lights incident simultaneously on the slab PC. We diagonalize the S matrix to obtain the eigenphase shifts, which determine the phase changes of the incident light passing through or reflecting back from the system. Conceptually, the scattering phase shift of an external probe relative to its free-space propagation is a standard quantity used to examine a target black box (for example, the Friedel sum rule for the screening of an impurity potential by electron cloud[5]). The formula of the DOS of PB's derived in this paper is expressed by the frequency derivative of the sum of the eigenphase shifts. The derivation of the DOS formula is given for a general case in which an arbitrary number of diffracted lights emerge simultaneously from a PC slab. Such a general treatment is important because the presence of diffraction characterizes the light scattering from PC's. Although the method proposed here to derive the DOS of PB's is applicable only to the leaky modes, its usefulness is obvious in the practical applications of PC's; any PB mode to be excited by an external light or to be used as a source of emitted light should be regarded as leaky in the sense that it is used through the coupling to the exterior free space. Some examples are light transmission and reflection in slab PC's,[6] extraction of laser light through PC surfaces,[7] and Smith-Purcell radiation from a charge traveling parallel to PC surfaces.[8–10] The efficiency of these phenomena depends critically on the lifetime of the leaky PB's involved. In other words, precise estimation of their lifetime is a crucial task in the physical and technological applications of PB's.

In Sec. II, we define the S matrix of a slab PC and derive the eigenvalue equation for the PB modes set up in it, taking into account their leakage. The formula is obtained in Sec. III for the increment of DOS due to the presence of a slab PC relative to that of free space by counting the number of solutions of the eigenvalue equation. An application of the derived formula is given in Sec. IV for a number of slab PC's of arrayed spheres. We illustrate there how to calculate the dispersion relation and lifetime of leaky PB's from the DOS profile. A brief summary is given in Sec. V.

II. SCATTERING MATRIX AND ITS EIGENVALUES

A. Definition of scattering channels

We consider a slab PC extending in the x,y direction with the origin of coordinates $\mathbf{r}=\mathbf{0}$ taken at its center. The period-

icity of the slab is assumed to be perfect in the lateral plane $-\infty<x,y<\infty$. We use a symbol $\mathbf{h}$ to denote a two-dimensional (2D) reciprocal lattice (RL) point in the xy plane. The vector $\mathbf{h}$ specifies a diffracted wave, reflected or transmitted. Let ω be the frequency and $\mathbf{k}$ the wave vector of an incident plane wave light. We make explicit the direction of propagation of a light by assigning a superscript $\pm$ to various quantities, and + to the quantities associated with the waves propagating to the $+z$ side of the slab from the $-z$ side. For example, the incident light of $\mathbf{k}^+$ ($\mathbf{k}^-$) stands for the light that is incident on the slab towards the $+z$ ($-z$) side; i.e., the light coming to the slab PC from below (above). Let $\mathbf{k}_\parallel$ be the component of the wave vector of $\mathbf{k}$ parallel to the xy plane, i.e.,

$$\mathbf{k}_\parallel = (k_x, k_y). \tag{1}$$

The translational invariance in the lateral plane shows that all the normal modes (actually they may be lifetime-broadened) of this system are specified by the lateral wave-vector components.

From the dispersion relation of light in free space,

$$\mathbf{k}^\pm = (\mathbf{k}_\parallel, \pm\Gamma_0) = (k_x, k_y, \pm\Gamma_0), \tag{2}$$

with

$$\Gamma_0 = \sqrt{\omega^2/c^2 - \mathbf{k}_\parallel^2}. \tag{3}$$

In the same way, the wave vector $\mathbf{k}_\mathbf{h}^\pm$ of diffracted light in the region outside the PC is defined to be

$$\mathbf{k}_\mathbf{h}^\pm = (\mathbf{k}_\parallel + \mathbf{h}, \pm\Gamma_\mathbf{h}), \tag{4}$$

with

$$\Gamma_\mathbf{h} \equiv \Gamma_\mathbf{h}(\omega) = \sqrt{\omega^2/c^2 - (\mathbf{k}_\parallel + \mathbf{h})^2}. \tag{5}$$

Only in the case in which

$$\omega > c|\mathbf{k}_\parallel + \mathbf{h}|, \tag{6}$$

$\mathbf{h}$ diffracted light comes out of the PC as plane wave light, which is observable at an observation point far from the PC. If Eq. (6) does not hold, the $\mathbf{h}$ wave is evanescent with a pure imaginary $\Gamma_\mathbf{h}$. We call the channel $\mathbf{h}$ of real $\Gamma_\mathbf{h}$ an open channel and $\mathbf{h}$ of imaginary $\Gamma_\mathbf{h}$ as a closed channel. For a fixed ω, each $\mathbf{h}$ defines one diffraction channel. All the channels other than those with smaller $|\mathbf{h}|$ are closed. The number of open channels at a given ω equals the number of $\mathbf{h}$'s that satisfy Eq. (6).

Let us suppose that we are in the frequency region where there are N diffraction channels open (one is the channel $\mathbf{h}=\mathbf{0}$). The incident light $\mathbf{k}^+$ coming from below the slab then gives rise to N transmitted lights (T lights) on the $+z$ side and N reflected lights (R lights) on the $-z$ side. Let

$$\mathbf{k}_{\mathbf{h}_1}^+, \mathbf{k}_{\mathbf{h}_2}^+, \ldots, \mathbf{k}_{\mathbf{h}_N}^+ \tag{7}$$

be the wave vectors of the T lights and

$$\mathbf{k}_{\mathbf{h}_1}^-, \mathbf{k}_{\mathbf{h}_2}^-, \ldots, \mathbf{k}_{\mathbf{h}_N}^- \tag{8}$$

be those of the R lights. Let $\mathbf{h}_1$ stand for the channel $\mathbf{h}=\mathbf{0}$, which is open for any ω.

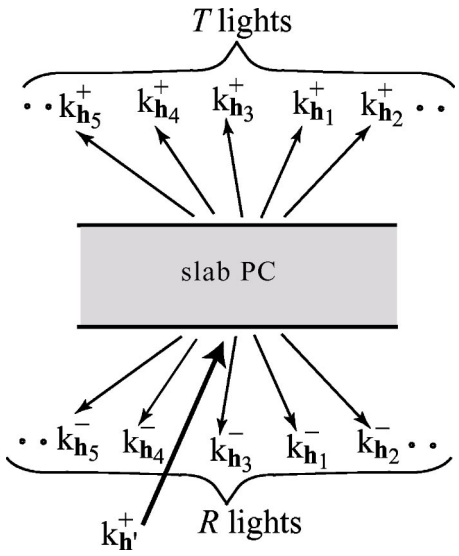

FIG. 1. T and R lights, both N in number, produced by an incident $\mathbf{k}_{\mathbf{h}'}^+$ light.

Suppose in an open channel $\mathbf{h}'$ we have an incident light of wave vector $\mathbf{k}_{\mathbf{h}'}^+$, which propagates towards the slab from below. This wave, too, is diffracted to produce T and R lights, each composed of N waves, as shown in Fig. 1. If the incident light has the form

$$\mathbf{a}_{\mathbf{h}'}^+ e^{i\mathbf{k}_{\mathbf{h}'}^+\cdot\mathbf{r}} \tag{9}$$

with a specified complex vector amplitude $\mathbf{a}_{\mathbf{h}'}^+$, it produces the T (R) lights of wave vector $\mathbf{k}_\mathbf{h}^+$ ($\mathbf{k}_\mathbf{h}^-$), which are expressed by

$$\mathbf{T}_{\mathbf{h}\mathbf{h}'}^{++} a_{\mathbf{h}'}^+ \exp(i\mathbf{k}_\mathbf{h}^-\cdot\mathbf{r}),$$

$$\mathbf{R}_{\mathbf{h}\mathbf{h}'}^{-+} a_{\mathbf{h}'}^+ \exp(i\mathbf{k}_\mathbf{h}^-\cdot\mathbf{r}). \tag{10}$$

The 3×3 tensor $\mathbf{T}_{\mathbf{h}\mathbf{h}'}^{++}$ of transmission describes the complex amplitude of the $\mathbf{h}$ wave in the process of the up-propagating $\mathbf{k}_{\mathbf{h}'}^+$ light being converted to the up-propagating $\mathbf{k}_\mathbf{h}^+$ wave. The tensor $\mathbf{R}_{\mathbf{h}\mathbf{h}'}^{-+}$ stands for the process of a $\mathbf{k}_{\mathbf{h}'}^+$ wave being reflected back as a $\mathbf{k}_\mathbf{h}^-$ wave. The element xy of, e.g., the tensor $\mathbf{T}_{\mathbf{h}\mathbf{h}'}^{++}$,

$$(\mathbf{T}_{\mathbf{h}\mathbf{h}'}^{++})_{xy},$$

is equal to the complex amplitude of the x component of the $\mathbf{k}_\mathbf{h}^+$ light, produced by a y-polarized $\mathbf{k}_{\mathbf{h}'}^+$ light that is incident on the PC with unit amplitude. For an incident amplitude $\mathbf{a}_{\mathbf{h}'}^+$, the x component of the reflected light with wave vector $\mathbf{k}_\mathbf{h}^-$ is given by

$$(\mathbf{R}_{\mathbf{h}\mathbf{h}'}^{-+}\mathbf{a}_{\mathbf{h}'}^+)_x = \sum_{i=x,y,z} (\mathbf{R}_{\mathbf{h}\mathbf{h}'}^{-+})_{xi} (\mathbf{a}_{\mathbf{h}'}^+)_i. \tag{11}$$

We will now consider the situation of the simultaneous incidence of the N plane waves. Let

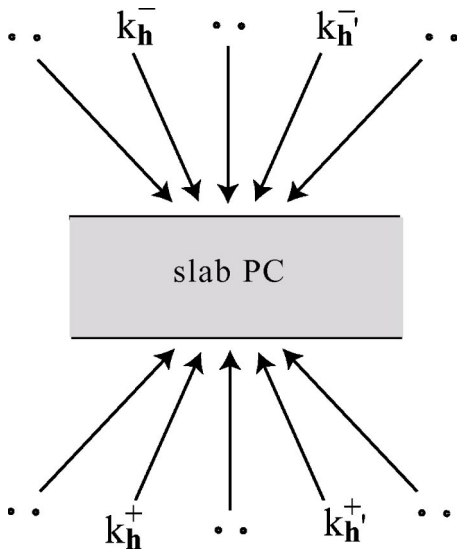

FIG. 2. Simultaneous incidence of N lights in the open channels from above and below the photonic crystal.

$$\mathbf{k}_{\mathbf{h}_1}^{+}, \mathbf{k}_{\mathbf{h}_2}^{+}, \ldots, \mathbf{k}_{\mathbf{h}_N}^{+}$$

and

$$\mathbf{k}_{\mathbf{h}_1}^{-}, \mathbf{k}_{\mathbf{h}_2}^{-}, \ldots, \mathbf{k}_{\mathbf{h}_N}^{-}$$

be the respective wave vectors of the incident lights from below and above the PC. This situation is shown in Fig. 2. This incidence condition still gives T and R lights, each composed of N plane waves. After the scattering by the PC of all these incident lights, the amplitude of the $\mathbf{k}_{\mathbf{h}}^{+}$ wave that appears on the $+z$ side of the PC has the form

$$\sum_{\mathbf{h}'} (\mathbf{T}_{\mathbf{hh}'}^{+} \mathbf{a}_{\mathbf{h}'}^{+} + \mathbf{R}_{\mathbf{hh}'}^{+-} \mathbf{a}_{\mathbf{h}'}^{-}), \tag{12}$$

where the summation over $\mathbf{h}'$ runs over open channels.

B. Flux conservation and *S* matrix

Here, we examine the conservation of the energy flow in the scattering event described above. We enclose the slab PC in a large box as shown in Fig. 3. The z component of the Poynting vector of the $\mathbf{k}_{\mathbf{h}}^{+}$ wave, i.e., the outflow of energy towards the $+z$ direction through the surface of the box in the $+z$ side, is

$$c\left(\frac{\Gamma_{\mathbf{h}}^{+}}{\omega/c}\right)\frac{\varepsilon_0}{2}$$

times the absolute square of the electric field; the quantity in the parentheses being the directional cosine of the outgoing wave vector $\mathbf{k}_{\mathbf{h}}^{+}$ with the z axis. If we consider the flux conservation for the Poynting vector averaged over one unit cell of the 2D lattice of a lateral plane, the interference terms between different $\mathbf{h}$'s disappear and the sum of the energy flows of all the open channels provides the total outflow in the $+z$ direction. Similarly, we can express the outflow in the $-z$ direction below the PC. The sum of the two then gives

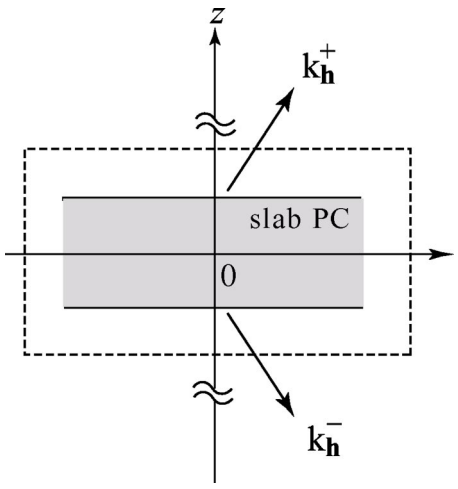

FIG. 3. A box surrounding the slab PC to consider the flux conservation between the incoming and outgoing lights.

$$[P_z^{+} - P_z^{-}]_{\text{outflow}} = \frac{\varepsilon_0}{2}\frac{c^2}{\omega}\sum_{\mathbf{h}} \Gamma_{\mathbf{h}} \left| \sum_{\mathbf{h}'} (\mathbf{T}_{\mathbf{hh}'}^{++} \mathbf{a}_{\mathbf{h}'}^{+} + \mathbf{R}_{\mathbf{hh}'}^{+-} \mathbf{a}_{\mathbf{h}'}^{-}) \right|^2 + \frac{\varepsilon_0}{2}\frac{c^2}{\omega}\sum_{\mathbf{h}} \Gamma_{\mathbf{h}} \left| \sum_{\mathbf{h}'} (\mathbf{R}_{\mathbf{hh}'}^{-+} \mathbf{a}_{\mathbf{h}'}^{+} + \mathbf{T}_{\mathbf{hh}'}^{--} \mathbf{a}_{\mathbf{h}'}^{-}) \right|^2. \tag{13}$$

Here, P_z^{+} and P_z^{-} are the z components of the Poynting vectors of the + waves and − waves, respectively. This quantity equals the energy inflow of the incident lights, which has the form

$$[P_z^{+} - P_z^{-}]_{\text{inflow}} = \frac{\varepsilon_0}{2}\frac{c^2}{\omega}\sum_{\mathbf{h}'} (\Gamma_{\mathbf{h}'} |\mathbf{a}_{\mathbf{h}'}^{+}|^2 + \Gamma_{\mathbf{h}'} |\mathbf{a}_{\mathbf{h}'}^{-}|^2) \tag{14}$$

in the simultaneous incidence.

In expressing the flux conservation

$$[P_z^{+} - P_z^{-}]_{\text{inflow}} = [P_z^{+} - P_z^{-}]_{\text{outflow}}, \tag{15}$$

which should hold for arbitrary incident amplitudes $\{\mathbf{a}_{\mathbf{h}'}^{+}\}$ and $\{\mathbf{a}_{\mathbf{h}'}^{-}\}$, various sums involved in both sides obviously imply the convenience of matrix notation. The matrices are introduced with their rows and columns labeled by $3N$ indices of $\mathbf{h}$ and x, y, and z. For example, a $3N \times 3N$ matrix $\mathbf{T}^{++}$ is formed by arraying 3×3 blocks $\mathbf{T}_{\mathbf{hh}'}^{++}$, etc. The freedoms of ± channels for each $\mathbf{h}$ are covered by adding two indices of ±. As a result, we deal with the matrices of dimension $6N \times 6N$. Then, the flux conservation Eq. (15), as combined with the arbitrariness of the incident amplitudes, turns out to be

$$[\hat{\mathbf{S}}']^{\dagger} \hat{\mathbf{\Gamma}}' \hat{\mathbf{S}}' = \hat{\mathbf{\Gamma}}', \tag{16}$$

where the dagger stands for the hermitian conjugate. Here $6N \times 6N$ matrices $\hat{\mathbf{S}}'$ and $\hat{\mathbf{\Gamma}}'$ are defined by

$$\hat{\mathbf{S}}' = \begin{pmatrix} \mathbf{T}^{++} & \mathbf{R}^{+-} \\ \mathbf{R}^{-+} & \mathbf{T}^{--} \end{pmatrix}, \tag{17}$$

with $3N \times 3N$ matrices $\mathbf{T}^{\pm\pm}$ and $\mathbf{R}^{\pm\mp}$ and

$$\hat{\mathbf{\Gamma}}' = \begin{pmatrix} \mathbf{\Gamma} & \mathbf{0} \\ \mathbf{0} & \mathbf{\Gamma} \end{pmatrix}, \tag{18}$$

the $3N \times 3N$ matrix $\mathbf{\Gamma}$ being a diagonal matrix formed by $\Gamma_{\mathbf{h}} \delta_{\mathbf{hh}'}$. The concrete forms for them are given in Appendix A.

Finally, we define matrix $\hat{\mathbf{S}}$ by

$$\hat{\mathbf{S}} = [\hat{\mathbf{\Gamma}}']^{1/2}\, \hat{\mathbf{S}}'\, [\hat{\mathbf{\Gamma}}']^{-1/2}. \tag{19}$$

An explicit form of the $(\mathbf{h}+, \mathbf{h}'-)$ block of $\hat{\mathbf{S}}$ is

$$[\hat{\mathbf{S}}]^{+-}_{\mathbf{hh}'} = \mathbf{\Gamma}_{\mathbf{h}}{}^{1/2} [\mathbf{R}^{+-}]_{\mathbf{hh}'} \mathbf{\Gamma}_{\mathbf{h}'}{}^{-1/2}. \tag{20}$$

The $(\mathbf{h}-, \mathbf{h}'+)$, $(\mathbf{h}+, \mathbf{h}'+)$, and $(\mathbf{h}-, \mathbf{h}'-)$ blocks of the S matrix are given by replacing $\mathbf{R}^{+-}$ of this equation by $\mathbf{R}^{-+}$, $\mathbf{T}^{++}$, and $\mathbf{T}^{--}$, respectively, according to the definition of $\hat{\mathbf{S}}'$ [Eq. (17)].

The flux conservation expressed by Eq. (16) is now rewritten compactly as

$$\hat{\mathbf{S}}^{\dagger} \hat{\mathbf{S}} = \mathbf{I}. \tag{21}$$

The matrix $\hat{\mathbf{S}}$ is thus a $6N \times 6N$ unitary matrix. Therefore, it has $6N$ eigenvalues of the form $e^{2i\delta^{(j)}}$ $(j = 1, 2, \ldots, 6N)$ with a real phase $\delta^{(j)}$. The matrix element of S,

$$S_{\mathbf{h}'+x, \mathbf{h}-y},$$

for example, is a complex scattering amplitude in the process of the incident light of unit amplitude of $(\mathbf{h}, -, y)$ [a y-polarized light in the $(\mathbf{h}-)$ channel] exiting out of the PC as an $(\mathbf{h}', +, x)$ light. We call $\delta^{(j)}$ an eigenphase shift. For $N = 1$, i.e., when only a direct transmitted light and a specularly reflected light of $\mathbf{h} = \mathbf{0}$ are produced by an incident light, we have six eigenphase shifts. We should have four eigenphase shifts instead of six, because we are dealing with the scattering of the incident *transverse* waves that give rise to *transverse* outgoing waves after the scattering.[11] This implies that out of six eigenphase shifts, two are meaningless. In the general case of N open channels, having $6N$ eigenphase shifts from a $6N \times 6N$ matrix $\mathbf{S}$, $2N$ out of $6N$ eigenphase shifts are meaningless; they appear due to the longitudinal component of polarization.

Such irrelevant eigenphase shifts had better be eliminated from a practical point of view. For this purpose, the local coordinate systems defined in reference to each of the open channels are convenient. For a wave of channel $(\mathbf{h}+)$ or $(\mathbf{h}-)$, we define the right-handed system {123} using the three orthonormal vectors

$$[\mathbf{e}_{\mathbf{h}}^{\pm}(1), \mathbf{e}_{\mathbf{h}}^{\pm}(2), \mathbf{e}_{\mathbf{h}}^{\pm}(3)], \tag{22}$$

$\mathbf{e}_{\mathbf{h}}^{+}(1)$ and $\mathbf{e}_{\mathbf{h}}^{+}(2)$ being perpendicular to $\mathbf{k}_{\mathbf{h}}^{+}$ and $\mathbf{e}_{\mathbf{h}}^{+}(3)$ being parallel to it. Thus, component 3 stands for the longitudinal polarization of $\mathbf{k}_{\mathbf{h}}^{+}$ light and axis 2 is always taken to be in the lateral plane, irrespective of $\mathbf{h}$. For the {123} coordinates of the $(\mathbf{h}-)$ channel, we choose three orthonormal vectors $\mathbf{e}_{\mathbf{h}}^{-}(i)$ $(i = 1, 2, 3)$ to be the mirror images of $\mathbf{e}_{\mathbf{h}}^{+}(i)$. Note that the {123} system differs from one channel to another. In this sense, we call the {123} system a local coordinate system.

We may then rewrite the S matrix using the 1 and 2 components of each channel in place of x, y, z components. The actual procedure is given in Appendix B. This procedure removes all the longitudinal components, and we are left with a 2×2 matrix, which is denoted as $\hat{\mathbf{T}}^{++}_{\mathbf{hh}'}$, etc. By arranging $\hat{\mathbf{T}}^{++}_{\mathbf{hh}'}$, $\hat{\mathbf{R}}^{+-}_{\mathbf{hh}'}$, etc., according to the channel labels, we may construct a $4N \times 4N$ S matrix. Let us denote the matrix thus obtained as $\mathbf{S}$

$$\mathbf{S} = \begin{pmatrix} \hat{\mathbf{T}}^{++} & \hat{\mathbf{R}}^{+-} \\ \hat{\mathbf{R}}^{-+} & \hat{\mathbf{T}}^{--} \end{pmatrix}, \tag{23}$$

where $\hat{\mathbf{T}}^{++}$ are block matrices formed by the array of 2×2 matrix $\hat{\mathbf{T}}^{++}_{\mathbf{hh}'}$. Hereafter, we call $\mathbf{S}$ the S matrix.

When $\mathbf{S}$ operates on a $4N$-dimensional column vector composed of the incident amplitudes of open channels (expressed in the local coordinates), Eq. (12) shows that the result is the transmitted and reflected amplitudes produced by the simultaneous incidence in all the open channels. The eigenvalues of $\mathbf{S}$ are obtained by the equation

$$\mathbf{S}\mathbf{v}^{(j)} = \lambda^{(j)} \mathbf{v}^{(j)}, \tag{24}$$

with

$$\lambda^{(j)} = e^{2i\delta^{(j)}}, \tag{25}$$

for $j = 1, 2, \ldots, 4N$. Explicitly, the eigenvector $\mathbf{v}^{(j)}$, a $4N$-dimensional column vector, has the form

$$(\mathbf{v}^{(j)})^{\mathrm{t}} = [v^{(j)}_{\mathbf{h}_1{}^+}(1), v^{(j)}_{\mathbf{h}_1{}^+}(2), \ldots, v^{(j)}_{\mathbf{h}_n{}^+}(1), v^{(j)}_{\mathbf{h}_n{}^+}(2), v^{(j)}_{\mathbf{h}_1{}^-}(1),$$

$$v^{(j)}_{\mathbf{h}_1{}^-}(2), \ldots, v^{(j)}_{\mathbf{h}_n{}^-}(1), v^{(j)}_{\mathbf{h}_n{}^-}(2)]. \tag{26}$$

The form of the transposed vector of $\mathbf{v}^{(j)}$ has been given with (1) and (2) specifying two transverse components of each channel. Note that $\mathbf{S}$ and hence $\lambda^{(j)}$ and $\mathbf{v}^{(j)}$ all depend on $\mathbf{k}_{\parallel}$. For simplicity, we use the symbols $\mathbf{S}$, $\lambda^{(j)}$ and $\mathbf{v}^{(j)}$ without adding the suffix $\mathbf{k}_{\parallel}$ to indicate the $\mathbf{k}_{\parallel}$ dependence.

The purpose of introducing $\delta^{(j)}$ for the eigenvalue $\lambda^{(j)}$ in Eqs. (24) and (25) is to express the frequencies of normal-modes and hence their DOS by using the eigenphase shifts. To proceed further, we assume the mirror symmetry with respect to the xy plane. Most artificially fabricated PC's belong to this category.

When the xy plane is a mirror plane (for the case of no mirror symmetry, see the comment at the end of this section), we can classify the modes by their parities of this mirror reflection. Since $\mathbf{S}$ commutes with this mirror operation, we have even- and odd-parity modes with the property of the eigenvector given by

$$v^{(j)}_{\mathbf{h}_l{}^+}(1) = v^{(j)}_{\mathbf{h}_l{}^-}(1), v^{(j)}_{\mathbf{h}_l{}^+}(2) = v^{(j)}_{\mathbf{h}_l{}^-}(2), \quad (l = 1 - N)$$

for even-parity modes,

$$v^{(j)}_{\mathbf{h}_l^+}(1) = -v^{(j)}_{\mathbf{h}_l^-}(1), v^{(j)}_{\mathbf{h}_l^+}(2) = -v^{(j)}_{\mathbf{h}_l^-}(2), \quad (l = 1-N)$$

for odd-parity modes. (27)

Let us assign the index $j=1,2,\ldots,2N$ to the even-parity modes and $j=2N+1,2N+2,\ldots,4N$ to the odd-parity modes. From now on, we shall focus on the even-parity modes.

Equations (24) and (25) imply the following. We let the wave

$$\mathbf{v}^{(j)}_{\mathbf{h}^-} e^{i\mathbf{k}^-_{\mathbf{h}}\cdot\mathbf{r}} = \begin{pmatrix} v^{(j)}_{\mathbf{h}^-}(1) \\ v^{(j)}_{\mathbf{h}^-}(2) \end{pmatrix} e^{i\mathbf{k}^-_{\mathbf{h}}\cdot\mathbf{r}} \tag{28}$$

propagate to the PC from above in the channel $(\mathbf{h}-)$ and another wave

$$\mathbf{v}^{(j)}_{\mathbf{h}^+} e^{i\mathbf{k}^+_{\mathbf{h}}\cdot\mathbf{r}} = \begin{pmatrix} v^{(j)}_{\mathbf{h}^+}(1) \\ v^{(j)}_{\mathbf{h}^+}(2) \end{pmatrix} e^{i\mathbf{k}^+_{\mathbf{h}}\cdot\mathbf{r}} \tag{29}$$

propagate from below in the channel $(\mathbf{h}+)$ [see Eq. (26) for the definition of $\mathbf{v}^{(j)}_{\mathbf{h}^+}$ and $\mathbf{v}^{(j)}_{\mathbf{h}^-}$]. Suppose they are sent to the PC simultaneously with the waves of the other channels, specified, similarly by the jth eigenvector, as shown in Fig. 2. Since their amplitudes are set so that as a whole, they constitute the jth eigenvector $\mathbf{v}^{(j)}$ of $\mathbf{S}$, the wave of any channel exits the PC after having acquired only a common phase change $2\delta^{(j)}$. Thus, for stationary wave propagation, the electric field of a channel $\mathbf{h}$ *above* the slab turns out to be

$$\mathbf{v}^{(j)}_{\mathbf{h}^-} e^{i\mathbf{k}^-_{\mathbf{h}}\cdot\mathbf{r}} + e^{2i\delta^{(j)}}\mathbf{v}^{(j)}_{\mathbf{h}^+} e^{i\mathbf{k}^+_{\mathbf{h}}\cdot\mathbf{r}} = e^{i\delta^{(j)}}\mathbf{v}^{(j)}_{\mathbf{h}^+} e^{i(\mathbf{k}_\parallel+\mathbf{h})\cdot\boldsymbol{\rho}}\cos(\Gamma_{\mathbf{h}} z + \delta^{(j)}), \tag{30}$$

where $\boldsymbol{\rho}=(x,y)$. The first term expresses the incident light of Eq. (28) and the second is the light produced by the PC. Similarly, we find below the slab

$$\mathbf{v}^{(j)}_{\mathbf{h}^+} e^{i\mathbf{k}^+_{\mathbf{h}}\cdot\mathbf{r}} + e^{2i\delta^{(j)}}\mathbf{v}^{(j)}_{\mathbf{h}^-} e^{i\mathbf{k}^-_{\mathbf{h}}\cdot\mathbf{r}} = e^{i\delta^{(j)}}\mathbf{v}^{(j)}_{\mathbf{h}} e^{i(\mathbf{k}_\parallel+\mathbf{h})\cdot\boldsymbol{\rho}}\cos(-\Gamma_{\mathbf{h}} z + \delta^{(j)}). \tag{31}$$

The property of even-parity modes, $\mathbf{v}^{(j)}_{\mathbf{h}^+}=\mathbf{v}^{(j)}_{\mathbf{h}^-}(\equiv\mathbf{v}^{(j)}_{\mathbf{h}})$ was used in Eqs. (30) and (31). Combining them, we find that the field of the channel $\mathbf{h}$ outside the slab has the form

$$e^{i\delta^{(j)}}\mathbf{v}^{(j)}_{\mathbf{h}} e^{i(\mathbf{k}_\parallel+\mathbf{h})\cdot\boldsymbol{\rho}}\cos(\Gamma_{\mathbf{h}}|z| + \delta^{(j)}). \tag{32}$$

This expression, which has the form of a standing wave, is valid both above and below the PC and suits our purpose of determining the eigenvalues.

C. Boundary condition and frequencies of normal modes

To obtain the eigenvalues, we put the PC slab symmetrically between two perfect mirrors, as shown in Fig. 4. We place the mirrors at $z=\pm L$. To determine the normal modes of the whole space of $-L<z<+L$, which has the PC at the center, we impose the boundary condition that the lateral components of the electric field vanish at the mirrors.

To find a solution subject to this boundary condition, we superpose Eq. (32) over j and $\mathbf{h}$, as

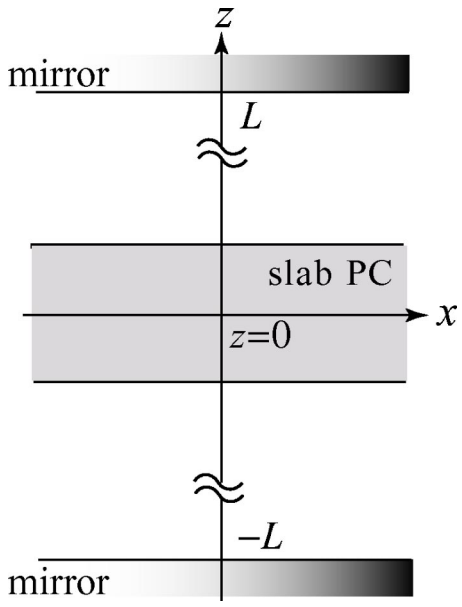

FIG. 4. Two parallel mirrors placed at $z=\pm L$ to consider the Fabry-Perot normal modes. We compare the number of the normal modes set up between the mirrors with and without the slab PC placed at $z=0$.

$$\mathbf{E}(\mathbf{r}) = \sum_{\mathbf{h}=\mathbf{h}_1}^{\mathbf{h}_N}\sum_{j=1}^{2N} e^{i\delta^{(j)}}\mathbf{v}^{(j)}_{\mathbf{h}} e^{i(\mathbf{k}_\parallel+\mathbf{h})\cdot\boldsymbol{\rho}}\cos(\Gamma_{\mathbf{h}}|z| + \delta^{(j)})C_j, \tag{33}$$

with unknown coefficients C_j, which we determine so that $\mathbf{E}(\mathbf{r})$ satisfies the boundary condition. The lateral components are x and y, and they are obtained by returning from the local coordinates to the fixed coordinates, which are obtained by using the inverse of the matrix $\mathbf{R}^{\pm}_{\mathbf{h}}$ given by Eq. (B1). Retaining a 2×2 block of matrix $(\mathbf{R}^{\pm}_{\mathbf{h}})^{-1}$ for conversion from $(1,2)$ to (x,y), we denote it as $\mathbf{r}^+_{\mathbf{h}}$. The procedure of Appendix B then leads to

$$\begin{pmatrix} E_x(\mathbf{r}) \\ E_y(\mathbf{r}) \end{pmatrix} = \sum_{\mathbf{h}=\mathbf{h}_1}^{\mathbf{h}_N}\sum_{j=1}^{2N} e^{i\delta^{(j)}}\mathbf{r}^+_{\mathbf{h}}\mathbf{v}^{(j)}_{\mathbf{h}} e^{i(\mathbf{k}_\parallel+\mathbf{h})\cdot\boldsymbol{\rho}}\cos(\Gamma_{\mathbf{h}}|z| + \delta^{(j)})C_j, \tag{34}$$

the product $\mathbf{r}^+_{\mathbf{h}}\mathbf{v}^{(j)}_{\mathbf{h}}$ giving a column vector composed of the x and y components of $\mathbf{v}^{(j)}_{\mathbf{h}}$. The right-hand side of this equation should vanish at the mirror surfaces at $z=\pm L$. Since the plane waves $e^{i(\mathbf{k}_\parallel+\mathbf{h})\cdot\boldsymbol{\rho}}$ of different $\mathbf{h}$'s are linearly independent, it then follows that

$$\sum_{j=1}^{2N} e^{i\delta^{(j)}}\mathbf{r}^+_{\mathbf{h}}\mathbf{v}^{(j)}_{\mathbf{h}}\cos(\Gamma_{\mathbf{h}}L + \delta^{(j)})C_j = \mathbf{r}^+_{\mathbf{h}}\begin{pmatrix} \sum_{j=1}^{2N} e^{i\delta^{(j)}}v^{(j)}_{\mathbf{h}}(1)\cos(\Gamma_{\mathbf{h}}L + \delta^{(j)})C_j \\ \sum_{j=1}^{2N} e^{i\delta^{(j)}}v^{(j)}_{\mathbf{h}}(2)\cos(\Gamma_{\mathbf{h}}L + \delta^{(j)})C_j \end{pmatrix} = 0 \tag{35}$$

for all $\mathbf{h}$. As the determinant of the 2×2 matrix $\mathbf{r}^+_{\mathbf{h}}$ is not zero, the column vector of this equation should vanish.

Finally, the condition for any open channel **h** leads to

$$\begin{array}{c} \\ \mathbf{h}_1 \\ \mathbf{h}_1 \\ \mathbf{h}_2 \\ \mathbf{h}_2 \\ \vdots \\ \vdots \\ \mathbf{h}_N \end{array} \begin{array}{c} \begin{array}{cccc} j=1 & & 2 & \cdots \end{array} \\ \begin{pmatrix} e^{i\delta^{(1)}} v^{(1)}_{\mathbf{h}_1}(1)\cos(\Gamma_{\mathbf{h}_1}L+\delta^{(1)}) & e^{i\delta^{(2)}} v^{(2)}_{\mathbf{h}_1}(1)\cos(\Gamma_{\mathbf{h}_1}L+\delta^{(2)}) & \cdots \\ e^{i\delta^{(1)}} v^{(1)}_{\mathbf{h}_1}(2)\cos(\Gamma_{\mathbf{h}_1}L+\delta^{(1)}) & e^{i\delta^{(2)}} v^{(2)}_{\mathbf{h}_1}(2)\cos(\Gamma_{\mathbf{h}_1}L+\delta^{(2)}) & \cdots \\ e^{i\delta^{(1)}} v^{(1)}_{\mathbf{h}_2}(1)\cos(\Gamma_{\mathbf{h}_2}L+\delta^{(1)}) & e^{i\delta^{(2)}} v^{(2)}_{\mathbf{h}_2}(1)\cos(\Gamma_{\mathbf{h}_2}L+\delta^{(2)}) & \cdots \\ e^{i\delta^{(1)}} v^{(1)}_{\mathbf{h}_2}(2)\cos(\Gamma_{\mathbf{h}_2}L+\delta^{(1)}) & e^{i\delta^{(2)}} v^{(2)}_{\mathbf{h}_2}(2)\cos(\Gamma_{\mathbf{h}_2}L+\delta^{(2)}) & \cdots \\ \cdots & \cdots & \cdots \\ \cdots & \cdots & \cdots \\ \vdots & \vdots & \ddots \end{pmatrix} \end{array} \begin{pmatrix} C_1 \\ C_2 \\ C_3 \\ \vdots \\ C_j \\ \vdots \\ C_{2N} \end{pmatrix} = 0. \tag{36}$$

This equation reveals that the index j of the eigenvalue of **S** cannot, in general, be the index to specify the normal modes. Rather, the combined effect of all j determines the normal modes. If it were not for the sum over j in Eq. (33), we would have obtained the eigenvalue equation from Eq. (35) as

$$\cos(\Gamma_{\mathbf{h}}L + \delta^{(j)}) = 0, \tag{37}$$

for a single j. This equation should be satisfied simultaneously for all **h**'s by the eigenvalue of ω. This is indeed impossible, for a solution for ω of Eq. (37) of a particular **h** depends on that **h** and it cannot in general satisfy Eq. (37) for the other open channels.

We have so far concentrated on the even-parity solutions, constructed by using the even-parity eigenphase shifts $j=1,2,\ldots,2N$. For the odd-parity eigenphase shifts $j=2N+1,2N+2,\ldots,4N$, an analysis similar to the above leads to an odd-parity secular equation, which is given by Eq. (36) with the cosines all replaced by sines.

When the mirror symmetry is absent in the slab, a superposition of even and odd modes constitutes a solution. In this case, the phase space of $j=1,2,\ldots,2N$ and that of $j=2N+1,2N+2,\ldots,4N$ no longer decouple. Extension to this less symmetric case is similarly carried out. Our remaining task is to count the number of solutions of Eq. (36) in a given frequency range.

III. CHANGE OF DENSITY OF STATES

Let us denote the matrix appearing in Eq. (36) of the even-parity modes as **M**. The eigenvalues for the normal modes are obtained from

$$\det \mathbf{M} = 0. \tag{38}$$

We can eliminate from **M** the factors that are irrelevant in determining the eigenvalues. First, we divide each of the columns by

$$e^{i\delta^{(1)}}, e^{i\delta^{(2)}}, \ldots. \tag{39}$$

We further eliminate the factor $\cos\Gamma_{\mathbf{h}}L$ from the **h**th row and $\cos\delta^{(j)}$ from the jth column of the matrix **M**, making use of

$$\cos(\Gamma_{\mathbf{h}}L + \delta^{(j)}) = \cos\Gamma_{\mathbf{h}}L\,\cos\delta^{(j)}[1 - \tan\Gamma_{\mathbf{h}}L\,\tan\delta^{(j)}]$$

in Eq. (36). These factors can be removed because they are independent either of the phase shifts $\delta^{(1)}, \delta^{(2)}, \ldots$ or the size L of the boundary condition: the eigenvalues ω must depend on them both in view of the induced shifts of frequency from the free-space values. By this procedure, we are left with

$$\det \mathbf{M} = 0 \rightarrow \det \mathbf{M}' = 0, \tag{40}$$

where

$$\mathbf{M}' = \begin{pmatrix} v^{(1)}_{\mathbf{h}_1}(1)(1-\tan\Gamma_{\mathbf{h}_1}L\,\tan\delta^{(1)}) & v^{(2)}_{\mathbf{h}_1}(1)(1-\tan\Gamma_{\mathbf{h}_1}L\,\tan\delta^{(2)}) & \cdots \\ v^{(1)}_{\mathbf{h}_1}(2)(1-\tan\Gamma_{\mathbf{h}_1}L\,\tan\delta^{(1)}) & v^{(2)}_{\mathbf{h}_1}(2)(1-\tan\Gamma_{\mathbf{h}_1}L\,\tan\delta^{(2)}) & \cdots \\ v^{(1)}_{\mathbf{h}_2}(1)(1-\tan\Gamma_{\mathbf{h}_2}L\,\tan\delta^{(1)}) & v^{(2)}_{\mathbf{h}_2}(1)(1-\tan\Gamma_{\mathbf{h}_2}L\,\tan\delta^{(2)}) & \cdots \\ v^{(1)}_{\mathbf{h}_2}(2)(1-\tan\Gamma_{\mathbf{h}_2}L\,\tan\delta^{(1)}) & v^{(2)}_{\mathbf{h}_2}(2)(1-\tan\Gamma_{\mathbf{h}_2}L\,\tan\delta^{(2)}) & \cdots \\ \cdots & \cdots & \cdots \\ \cdots & \cdots & \cdots \\ \vdots & \vdots & \ddots \end{pmatrix}. \tag{41}$$

The poles of the factors

$$\tan \Gamma_{\mathbf{h}_1} L,\ \tan \Gamma_{\mathbf{h}_2} L, \ldots$$

of $\mathbf{M}'$ or the solutions of $\cos \Gamma_{\mathbf{h}} L = 0$ in the complex ω plane, give even-parity eigenvalues of photons in the free space bounded by the mirrors. Therefore, we conclude that the eigenvalues perturbed by the presence of the PC are given by the zeros of $\det \mathbf{M}'$, while the unperturbed eigenvalues in the absence of the PC are given by the poles of $\det \mathbf{M}'$. Thus, the increment of the number of the normal modes due to the presence of the slab PC in a frequency interval is given by the number of poles therein minus the number of zeros.

From the theory of complex function (see Ref. 12, for example), the increment of the number of modes of wave vector $\mathbf{k}_\parallel$ in the frequency interval $[\omega_0, \omega]$, denoted as $\Delta N_{\mathbf{k}_\parallel}(\omega_0; \omega)$, is given by

$$\Delta N_{\mathbf{k}_\parallel}(\omega_0; \omega) = -\frac{1}{\pi} \mathrm{Im}\left[\log \frac{\det \mathbf{M}'(\omega + i\varepsilon)}{\det \mathbf{M}'(\omega_0 + i\varepsilon)} \right], \qquad (42)$$

where $\mathrm{Im}[\cdots]$ stands for the imaginary part of $[\cdots]$ and $+i\epsilon$ ($\epsilon = +0$) shows that the logarithms are evaluated on the upper edge of the branch cut on the real ω axis. The change of DOS at the frequency ω, denoted by $\Delta\rho_{\mathbf{k}_\parallel}(\omega)$, is obtained by differentiating $\Delta N_{\mathbf{k}_\parallel}(\omega_0; \omega)$ with respect to ω.

It seems difficult to reduce $\det \mathbf{M}'$ further to obtain $\Delta\rho_{\mathbf{k}_\parallel}(\omega)$ because the dependences on the column index $\mathbf{h}$ and row index j are both present in the matrix elements of Eq. (41). In the special limit $L \to \infty$, however, we can proceed further to arrive at the final analytical expression. In this limit, we find (Appendix C)

$$\tan \Gamma_{\mathbf{h}}(\omega + i\epsilon) L \to i, \qquad (L \to \infty). \qquad (43)$$

Thus, from Eq. (41), we find

$$\det \mathbf{M}' = \det \begin{bmatrix} v^{(1)}_{\mathbf{h}_1}(1) & v^{(2)}_{\mathbf{h}_1}(1) & v^{(3)}_{\mathbf{h}_1}(1) & \cdots \\ v^{(1)}_{\mathbf{h}_1}(2) & v^{(2)}_{\mathbf{h}_1}(2) & v^{(3)}_{\mathbf{h}_1}(2) & \cdots \\ v^{(1)}_{\mathbf{h}_2}(1) & v^{(2)}_{\mathbf{h}_2}(1) & \cdots & \cdots \\ v^{(1)}_{\mathbf{h}_2}(2) & v^{(2)}_{\mathbf{h}_2}(2) & \cdots & \cdots \\ \vdots & \vdots & \vdots & \ddots \end{bmatrix} \times \prod_{j=1}^{2N} (1 - i \tan \delta^{(j)}). \qquad (44)$$

The first factor of the right-hand side is unity and can be removed. This property of the eigenvectors comes from the unitarity of the S matrix and the reality of the eigenvectors, the latter being guaranteed by the time reversal symmetry of the S matrix. Since

$$\mathrm{Im}\left[\log \prod_{j=1}^{2N} (1 - i \tan \delta^{(j)}) \right] = \sum_{j=1}^{2N} \mathrm{Im}[\log(1 - i \tan \delta^{(j)})] = -\sum_{j=1}^{2N} \delta^{(j)}, \qquad (45)$$

we find

$$\Delta\rho_{\mathbf{k}_\parallel}(\omega)^{(\mathrm{even})} = \frac{d}{d\omega} \Delta N_{\mathbf{k}_\parallel}(\omega_0; \omega) = -\frac{d}{d\omega} \frac{1}{\pi} \mathrm{Im}\left[\log \prod_{j=1}^{2N} (1 - i \tan \delta^{(j)}) \right] = \frac{1}{\pi} \sum_{j=1}^{2N} \frac{d\delta^{(j)}}{d\omega} \qquad (46)$$

for even-parity PB's. This is our final expression for the increment of DOS of even-parity PB's. We have assigned the superscript "even" to emphasize that. The expression for the odd-parity PB's is similar except that the odd-parity eigenphase shifts $\delta^{(j)}$ ($j = 2N+1, 2N+2, \ldots, 4N$) are used:

$$\Delta\rho_{\mathbf{k}_\parallel}(\omega)^{(\mathrm{odd})} = \frac{1}{\pi} \sum_{j=2N+1}^{4N} \frac{d\delta^{(j)}}{d\omega}. \qquad (47)$$

Altogether, we find

$$\Delta\rho_{\mathbf{k}_\parallel}(\omega) = \Delta\rho_{\mathbf{k}_\parallel}(\omega)^{(\mathrm{even})} + \Delta\rho_{\mathbf{k}_\parallel}(\omega)^{(\mathrm{odd})} = \frac{1}{\pi} \sum_{j=1}^{4N} \frac{d\delta^{(j)}}{d\omega}; \qquad (48)$$

i.e., the ω-derivative of the sum of the $4N$ eigenphase shifts gives the total change of DOS. This expression of the total increment is shown to be valid in the absence of the mirror symmetry in the xy plane of the PC.

IV. APPLICATION TO PHOTONIC CRYSTALS OF SPHERES ARRAYED IN A SQUARE LATTICE AND A SIMPLE CUBIC LATTICE

In this section, we apply the above formula to slab PC's of arrayed spheres. We examine 2D systems of dielectric spheres arrayed periodically. Based on Eqs. (46) and (47), we calculate the DOS for monolayer and stacked layer model PC's. We choose n, the refractive index of spheres, to be 1.44, having in mind polytetrafluoroethylene (PTFE)[13] spheres whose diameter is in the millimeter range, and let the ratio of radius a of spheres to lattice constant d be $a/d = 0.5$, for the system of spheres just in contact in the square lattice. These parameters correspond to the PC's, which were actually prepared and used to examine their optical properties experimentally in the millimeter wavelength region of light.[14]

Light scattering from a slab of arrayed dielectric spheres is treated precisely by the vector Korringa-Kohn-Rostoker (KKR) formalism[15–17] and layer KKR formalism,[6,17] which give us high-quality numerical data for the T and R lights and hence the S matrix defined by Eq. (23) for a prescribed $\mathbf{k}_\parallel$ value. All the eigenphase shifts are then obtained by numerically diagonalizing the S matrix. We emphasize that Eqs. (46) and (47) are general, not limited to systems of spheres, if only the amplitudes of T and R lights of all the open channels are calculated. We assume the square lattice of spheres in the lateral plane and the simple cubic lattice when the layers are stacked.

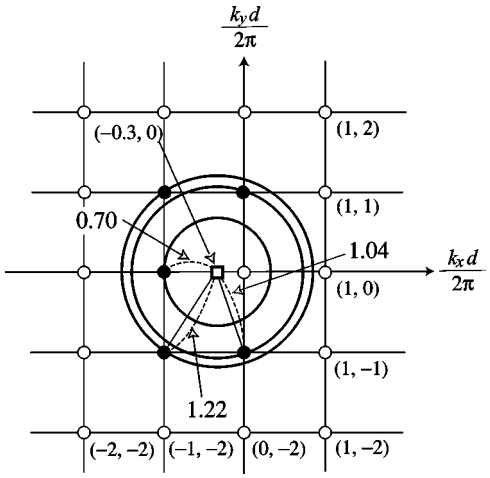

FIG. 5. Circles of radius ω and 2D reciprocal lattices (RL) in the $k_x k_y$ plane. The center of the circles shown by the open square is taken at $(k_x,k_y)(d/2\pi)=(-0.3,0)$, corresponding to the incident condition $\mathbf{k}_\parallel d/2\pi=(0.3,0)$ under study. The RL points of the square lattice are shown by open and solid points. Three circles are given to show the critical situations of channel opening, with the touching RL point of each case indicated by the filled lattice point.

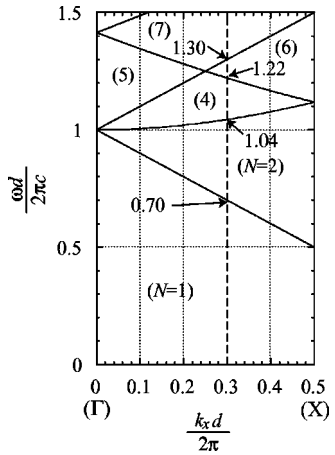

FIG. 6. Number of open 2D reciprocal lattice points as functions of ω and k_x, in the $\Gamma-X$ direction ($k_y=0$). The number N of the open RL points is given in parenthesis in each region. Three threshold values for $\omega d/2\pi c$ of channel opening are given for the case of $k_x d/2\pi=0.3$, corresponding to the three circles of Fig. 5.

First we study the monolayer system. This system was examined both theoretically and experimentally by Ohtaka *et al.*,[11] Kondo *et al.*[18] and Yano *et al.*[19] Theoretical analysis was also given for the DOS in the frequency region of no diffraction. In what follows, we investigate the increment of DOS for the lateral wave vector $\mathbf{k}_\parallel d/2\pi=(0.3,0)$, which was chosen arbitrarily.

Figure 5 depicts 2D RL points in the $k_x k_y$ plane, each specified by the point $(2\pi/d)(m,n)$ of the square lattice. A circle of radius ω is also shown with its center placed at $\mathbf{k}_\parallel d/2\pi=(-0.3,0)$. In the figure, circles of three different radii are drawn. From Eq. (5), the channel $\mathbf{h}$ opens when the radius increases with ω to cross the point $\mathbf{h}$. The number of the RL points inside the circle is equal to the number of open channels at ω.

For an incident light of frequency ω and wave vector $\mathbf{k}_\parallel$, we can imagine an Ewald sphere of radius ω in the $(k_x k_y k_z)$ space, whose center is placed at

$$[-\mathbf{k}_\parallel, -\sqrt{(\omega/c)^2-\mathbf{k}_\parallel^2}].$$

The vector drawn from this center to the origin $\mathbf{k}=0$ represents the incident wave vector $\mathbf{k}^+$. A circle of Fig. 5 may also be viewed as a locus of this Ewald sphere cut by the plane $k_z=-\sqrt{(\omega/c)^2-\mathbf{k}_\parallel^2}$, where the center is lying; in this picture, the lattice points of Fig. 5 are the horizontal view of the 2D reciprocal lattice *rods* arrayed parallel to z.

As ω increases in Fig. 5 with $k_x d/2\pi$ fixed at 0.3, the circle becomes larger, touching first the point $\mathbf{h}d/2\pi=(-1,0)$ at $\omega d/2\pi c=0.70$, when the diffracted T light of $\mathbf{k}_\mathbf{h}^+$ and R light of $\mathbf{k}_\mathbf{h}^-$ start to appear in channel $\mathbf{h}d/2\pi=(-1,0)$. The frequency $\omega d/2\pi c=1.044$ is for the second contact, when two additional channels, $\mathbf{h}d/2\pi=(0,1)$ and $(0,-1)$, open. The third (fourth) contact takes place at $\omega d/2\pi c=1.221$ (1.30). Figure 6 shows N, the number of open channels, in the (k_x,ω) plane for the incident light of $\mathbf{k}_\parallel=(k_x,0)$. The vertical dashed line corresponds to the case $(k_x,k_y)(d/2\pi)=(0.3,0)$, presented in Fig. 5.

In the frequency region $0<\omega d/2\pi c<0.70$, there is no diffraction ($N=1$) for $(k_x,k_y)(d/2\pi)=(0.3,0)$. We have one plane wave T light of a complex amplitude T_{00} and one R light of a complex amplitude R_{00}, representing directly transmitted light and specularly reflected light. The S matrix is 4×4, yielding four eigenphase shifts by diagonalization. They are p-polarized and s-polarized eigenmodes, both classified further into even and odd parities of the mirror reflection in the xy plane. The p and s modes decouple because our choice of $\mathbf{k}_\parallel$ to be directed along the Δ axis of the 2D Brillouin zone guarantees the mirror symmetry in the xz plane (the p mode is even and the s mode is odd). Analysis of Ref. 11 [Eqs. (A12) and (A15) thereof] proved that the sum of the four eigenphase shifts is equal to the sum of the phase of T_{00} of p-polarized incident light and that of s-polarized incident light for the frequency range of $N=1$. Namely, the phase of T_{00} of the p-polarized light is equal to the sum of $(p+)$ and $(p-)$ eigenphase shifts. The same holds true for T_{00} of s-polarized light. Therefore, the DOS formula defined in Ref. 11 is reproduced by the special case $N=1$ of the present general theory.

In the frequency region $\omega d/2\pi c\geqslant 0.70$, we enter the new regime of $N\geqslant 2$. We compare the calculated transmittance $|T_{00}|^2$ of the direct light with the DOS formula. We restrict ourselves to the response of the s-polarized incident light, because the discussion of the p incidence is similar.

Let us first examine what the previous DOS formula, valid only for $N=1$, yields in the case of $N\geqslant 2$. Namely, we plot the phase of T_{00} of s light as our DOS. Figure 7(a) shows the calculated $|T_{00}|^2$ for the s-light, and Fig. 7(b) shows the phase of the s-light T_{00}. Note that we can treat scalar T_{00} in obtaining the phase because the polarization of the directly transmitted light is the same as the incident light for $\mathbf{k}_\parallel$ along the Δ axis. There is perfect coincidence in the positions of the fine structures in Figs. 7(a) and 7(b). Conse-

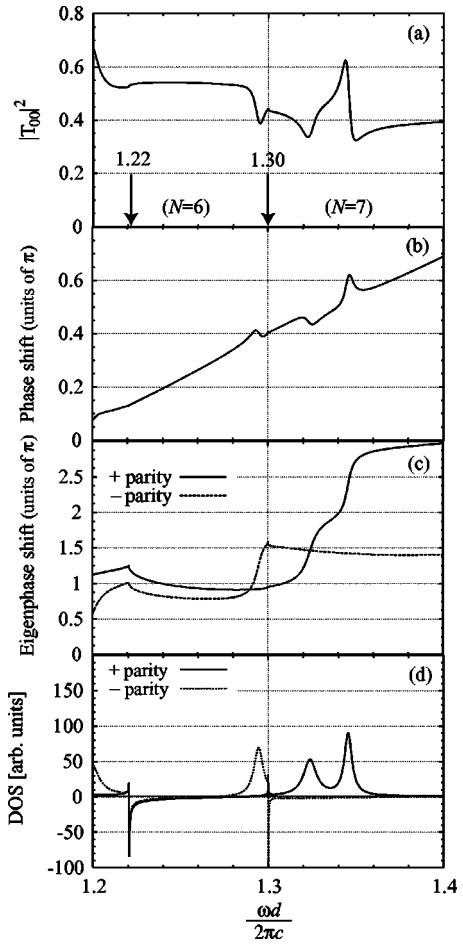

FIG. 7. Frequency dependence in the region $1.2<\omega d/2\pi c<1.4$ of transmittance and increment of DOS of *s*-polarized light with $(k_x,k_y)(d/2\pi)=(0.3,0)$. The calculation is made for a monolayer PC consisting of a square array of dielectric spheres, whose parameters are given in the text. Panel (a) shows the transmittance of the direct light ($\mathbf{h}=0$), defined by $|T_{00}|^2$. Two arrows indicate the threshold frequencies for the change of the number N of open channels, one from the case of $N=4$ to $N=6$ at $\omega d/2\pi c=1.22$ and the other from $N=6$ to $N=7$ at $\omega d/2\pi c=1.30$. See Fig. 5 for the values of the threshold frequency. Panel (b) shows the phase of the complex amplitude derived from $T_{00}/|T_{00}|$, which would yield a correct sum of the eigenphase shifts when $N=1$. Panel (c) shows the sum of the eigenphase shifts derived from the formula (48). Only the eigenphase shifts of *s*-polarized modes are retained. Panel (d) gives the correct DOS of the *s*-polarized PB's, which is defined by Eq. (48).

quently, the DOS formula valid for $N=1$ still works in the case $N\geqslant 2$ for simply determining the existence of PB's. However, we note that a correct DOS change due to the presence of a PB mode should be one; i.e., the sum of the phase shifts should change by π, whenever ω increases to cross a PB mode.[11] In Fig. 7(b), we see that the change of the phase shift at any fine structure is very short of π. (For comparison, in Fig. 8, we plot the situation seen in the region of $N=1$ to show that the procedure indeed works there.) The DOS of PB's and the leakage-induced lifetime estimated from Fig. 7(b) are hardly reliable. For example, peaks and humps of the curves of Fig. 7(b) produce singular line shapes in the DOS profile when differentiated according to Eqs. (46)

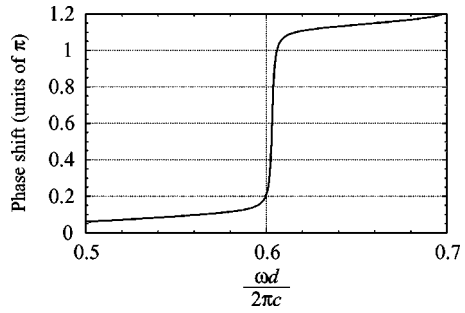

FIG. 8. Typical example of an abrupt phase change of the complex transmission amplitude. The phase obtained from $T_{00}/|T_{00}|$ is plotted in the frequency region of $N=1$. The light is *s*-polarized with $(k_x,k_y)(d/2\pi)=(0.3,0)$, incident on the monolayer PC used in Fig. 7. The change of the phase is just π.

and (47), quite different from Lorentzian shapes expected from the general theory of lifetime broadening. To summarize, the straightforward extension of the DOS formula of $N=1$ to the new region of $N\geqslant 2$ does not give correct information. This incorrect procedure using the previous DOS formula does not take proper account of diffracted waves. Therefore, we apply the present formula defined by Eqs. (46) and (47) to this condition.

Figure 7(c) depicts the sum of the eigenphase shifts

$$\sum_{j=1}^{4N}\delta^{(j)} \tag{49}$$

of Eq. (48), which we claim to be a correct formula for the increment of DOS. We can easily classify by inspection the whole set of eigenphase shifts into the *p*- and *s*-polarized modes by the numerically calculated eigenvectors of **S**. We retain in 7(c) only the phase shifts of *s*-polarized modes to obtain the DOS of *s*-active PB's, which is to be compared with the *s* transmittance $|T_{00}|^2$ given in (a). We display the sum of the phase shifts by dividing it into ± parities of the mirror symmetry with respect to the *xy* plane. Panel (c) obviously confirms that the sum of the eigenphase shifts corrects the insufficient magnitudes of the jumps at the excited PB modes shown in Fig. 7(b).

Figure 7(d) shows its ω derivative, the DOS of the PB's of $(k_x,k_y)(d/2\pi)=(0.3,0)$. The DOS profile consists of Lorentzian peaks, as it should, whose full width at half-maximum (FWHM) gives the inverse of the lifetime of the PB's. Any optical response of a PC is related more or less to its DOS profile and generally has a resonant enhancement accompanying a PB excitation. For example, the FWHM of excited PB modes primarily determines the emission spectrum from an atom in a PC. Three DOS peaks around $\omega d/2\pi c\simeq 1.3$ of Fig. 7(d) provide an estimate FWHM $=\Delta\omega d/2\pi c\simeq 0.01$, leading to an estimate of $Q=\omega/\Delta\omega \simeq 100$. The kinks seen at the frequencies of channel opening in Fig. 7(d) are interesting. The singular behavior of the spectrum associated with the channel opening has been historically named the Wood anomaly[20] and was analyzed in detail in quantum mechanics text book.[21] Various kinds of singularities, appearing often as sharp kinks but sometimes

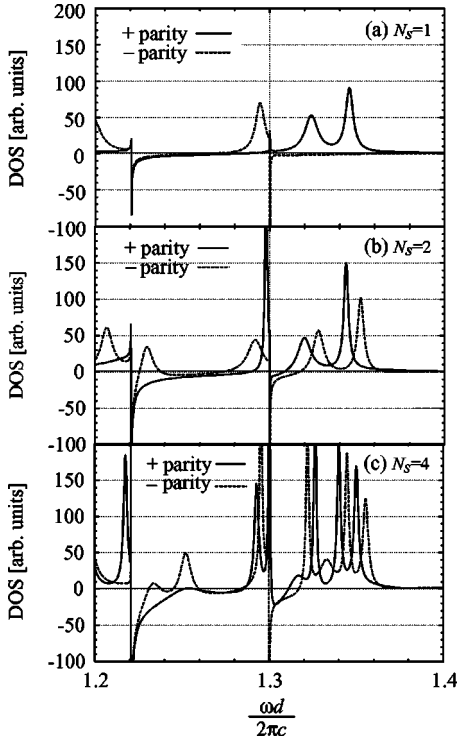

FIG. 9. Increment of DOS of a slab PC of stacked 2D layers as a function of frequency. N_s is the number of stacked layers. The result is given for PB's of s polarization with $(k_x,k_y)(d/2\pi)=(0.3,0)$. Panel (a) is a reproduction of Fig. 7(d) and shows the DOS of a monolayer PC ($N_s=1$). The solid (dashed) curve shows the even-parity (odd-parity) PB's. The Q values of PB's improve, or their lifetimes become longer and the density of the peaks increases, when N_s increases.

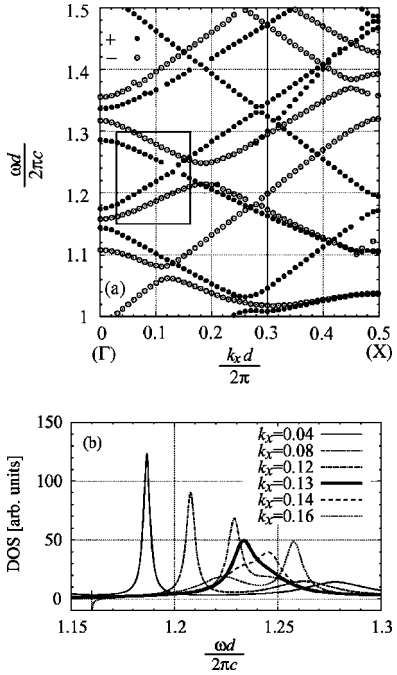

FIG. 10. Band structure and the wave-vector dependence of the DOS profile (s-polarized PB's). Panel (a) shows the band structure of a 2D PC (a monolayer array of spheres) along the $\Gamma-X$ axis in the 2D Brillouin zone. The parameters for the PC are the same as used above. The solid circles correspond to the even-parity modes of s polarization, while the dotted circles represent the odd-parity modes of s polarization. A vertical line is drawn at $k_x d/2\pi=0.3$, corresponding to the case examined in Fig. 7. Panel (b) shows how the width of a DOS peak depends on the band index and wave-vector. The phase space enclosed by the rectangle in (a) is examined in (b).

as dips or inflection points, are known to arise in the transmission spectrum. See Ref. 22 for the variety of singularities in the case of a PC. In Fig. 7(d), we have plotted the *increment* of DOS due to the presence of a slab PC and denoted it simply as DOS. Actually, therefore, a negative DOS of Fig. 7(d) just above the channel opening stands for a *decrease* of DOS. We believe the negative increment of DOS to be a genuine feature associated with Wood anomalies.

Next, we turn to the systems composed of stacked layers of arrayed PTFE spheres. Let N_s be the number of stacked layers. For this case, too, a theoretical analysis of DOS was given previously in the region of $N=1$.[19] In the bilayer system ($N_s=2$), the monolayer photonic bands of each of the two layers, which will be doubly degenerate if they are sufficiently far apart, are coupled to produce bonding and antibonding PB states.[23,24] Therefore, as N_s increases, the band population increases in a given frequency range. Figure 9 shows DOS obtained from our formulae [Eqs. (46) and (47)] for several N_s in the same frequency range and array of spheres as above. Except in the regions of channel opening, we can clearly see the bonding and antibonding splitting, when N_s becomes twice as large. The resonant optical response of a PB becomes sharper and sharper in accordance with the sharpening of DOS peaks as N_s increases. We can see that the DOS peaks for $N_s=4$ have their Q values several times larger than those in the system of $N_s=1$, estimated above to be about 100. In this way, we can quantitatively discuss the bonding and antibonding splitting of lifetime-broadened degenerate levels through the correct DOS formula and can calculate the Q values of the split levels as functions of N_s. These features are extensions of what was found previously in the frequency region of no diffraction.[25]

The plot of the positions of the DOS peaks as functions of $\mathbf{k}_\parallel$ gives the band structure of leaky PB's. Figure 10(a) illustrates the band structure for $\mathbf{k}_\parallel=(k_x,0)$, i.e., along the $\Gamma-X$ direction of the monolayer PC examined in Fig. 7. We show only the band structure of s-active PB's, derived from the s-active eigenphase shifts. The empty (filled) circles correspond to the modes with even (+) [odd (−)] parity with respect to the xy mirror symmetry. The general features of the calculated band structure are understandable using the band structure of an empty lattice. The similarity to an empty lattice stems from the fact that we have used a small refractive index $n=1.44$ in the analysis. For a PC of larger n, no problem arises except for a slower convergence in the calculation of the matrix $\mathbf{S}$, which, too, is overcome by the KKR formulation used here.

In the band structure of Fig. 10(a), there are some bands, with disconnected parts, which are too broad to produce a distinct peak there. Figure 10(b) illustrates this feature in the frequency region enclosed by the square in Fig. 10(a). The

DOS profiles for even-parity (+) modes with several values of k_x are given in Fig. 10(b), which shows that the lifetime of a leaky PB depends both on the wave vector k_x and the band index.[2,3,11] As k_x becomes larger, the two peaks approach and at $k_x d/2\pi=0.13$ they coalesce into a single broad peak, shown by the thick solid line. A further increase in k_x, however, resolves two modes again (e.g., the case of $k_x d/2\pi=0.16$). Near $k_x d/2\pi=0.13$, we cannot follow the two modes precisely.

V. SUMMARY

This paper presents a formula for the DOS of leaky PB's. The DOS of PB's in the leaky region of the phase space $(\omega, \mathbf{k}_\parallel)$ is a key factor that determines the magnitude of the resonant enhancement of optical signals from PC's, such as the emission cross-section of photons from an imbedded atom, for example.[26–30] In the DOS calculation, a complication arises from the need to take account of the presence of energy-carrying diffraction channels. We have shown that the DOS of leaky PB's of slab PC's is obtained from the complex transmission and reflection amplitudes of all the lights incident in the open channels and that it is expressed by the eigenphase shifts obtained by diagonalizing the S matrix defined using all the diffracted lights.

Based on the derived formula, we analyzed the transmittance of incident light for PC's of arrayed spheres and demonstrated that the extended definition of the scattering matrix given in this paper is very crucial in the frequency range where the diffraction channels are open. To show the usefulness of the formula, we have calculated the dispersion relations and lifetime of PB's from the DOS profile obtained for a model PC of arrayed spheres of finite thickness.

Recently, the local density of states (LDOS) of electromagnetic fields near the solid state surfaces is examined[31] and it is shown that the LDOS related to the surface states of a solid is accessible by scanning near-field spectroscopy images obtained experimentally. The LDOS at a point $\mathbf{r}$ is in essence the DOS times the squared eigenvectors at $\mathbf{r}$ of the electromagnetic normal modes. The genuine DOS of a system is thus a quantity which remains after integrating out the eigenvectors in the LDOS. It is thus determined solely by how the poles are distributed in the complex frequency space of electromagnetic Green's functions. The essence of the present paper is that the DOS in the leaky region is obtainable from the far-field amplitudes of incident light waves, in contrast to that of LDOS, which is related to the near-field information; the DOS is accessible by conventional measurements of the light transmission and reflection. This statement holds not only in slab PC's concerned in this paper, but also in ordinary solid state systems.

Since the formula requires only the complex amplitudes of the reflected and transmitted waves, its applicability is quite general and not limited to PC's of spheres.

ACKNOWLEDGMENTS

The present work is supported by "Promotion of Science and Technology" from the Ministry of Education, Sports, Culture, Science and Technology of Japan. This work is also supported by a Grant-in-Aid from the same ministry.

APPENDIX A: FORMS OF $3N\times3N$ MATRICES $\mathbf{T}^{++}$ AND $\mathbf{\Gamma}$

The $3N\times3N$ matrices $\mathbf{T}^{++}$ and $\mathbf{\Gamma}$ used in introducing the $6N\times6N$ matrices in Eqs. (17) and (18) are given here. The matrix $\mathbf{T}^{++}$ is defined by

$$\mathbf{T}^{++}=\begin{pmatrix} \mathbf{T}^{++}_{\mathbf{h}_1\mathbf{h}_1} & \mathbf{T}^{++}_{\mathbf{h}_1\mathbf{h}_2} & \mathbf{T}^{++}_{\mathbf{h}_1\mathbf{h}_3} & \cdots & \mathbf{T}^{++}_{\mathbf{h}_1\mathbf{h}_N} \\ \mathbf{T}^{++}_{\mathbf{h}_2\mathbf{h}_1} & \mathbf{T}^{++}_{\mathbf{h}_2\mathbf{h}_2} & \mathbf{T}^{++}_{\mathbf{h}_2\mathbf{h}_3} & \cdots & \mathbf{T}^{++}_{\mathbf{h}_2\mathbf{h}_N} \\ \mathbf{T}^{++}_{\mathbf{h}_3\mathbf{h}_1} & \mathbf{T}^{++}_{\mathbf{h}_3\mathbf{h}_2} & \mathbf{T}^{++}_{\mathbf{h}_3\mathbf{h}_3} & \cdots & \mathbf{T}^{++}_{\mathbf{h}_3\mathbf{h}_N} \\ \vdots & \vdots & \vdots & \ddots & \vdots \\ \mathbf{T}^{++}_{\mathbf{h}_N\mathbf{h}_1} & \mathbf{T}^{++}_{\mathbf{h}_N\mathbf{h}_2} & \mathbf{T}^{++}_{\mathbf{h}_N\mathbf{h}_3} & \cdots & \mathbf{T}^{++}_{\mathbf{h}_N\mathbf{h}_N} \end{pmatrix}. \quad \text{(A1)}$$

The 3×3 blocks $\mathbf{T}^{++}_{\mathbf{h}_1\mathbf{h}_2}$, etc., are introduced in Eq. (10). Other matrices $\mathbf{T}^{--}$, $\mathbf{R}^{+-}$, etc. are similarly defined using the $\mathbf{T}^{--}_{\mathbf{h}_1\mathbf{h}_2}$ and $\mathbf{R}^{+-}_{\mathbf{h}_1\mathbf{h}_2}$, respectively.

The $3N\times3N$ diagonal matrix $\mathbf{\Gamma}$ used in Eq. (18) is defined by

$$\mathbf{\Gamma}=\begin{pmatrix} \mathbf{\Gamma}_{\mathbf{h}_1} & 0 & 0 & \cdots & 0 \\ 0 & \mathbf{\Gamma}_{\mathbf{h}_2} & 0 & \cdots & 0 \\ 0 & 0 & \mathbf{\Gamma}_{\mathbf{h}_3} & \cdots & 0 \\ \vdots & \vdots & \vdots & \ddots & \vdots \\ 0 & 0 & 0 & \cdots & \mathbf{\Gamma}_{\mathbf{h}_N} \end{pmatrix}=\mathbf{\Gamma}_{\mathbf{h}_n}\delta_{\mathbf{h}_n\mathbf{h}_m}, \quad \text{(A2)}$$

where the 3×3 diagonal matrix $\mathbf{\Gamma}_{\mathbf{h}_n}$ is

$$\mathbf{\Gamma}_{\mathbf{h}_n}=\begin{array}{c} \\ x \\ y \\ z \end{array}\begin{array}{c} \begin{array}{ccc} x & y & z \end{array} \\ \begin{pmatrix} \Gamma_{\mathbf{h}_n} & 0 & 0 \\ 0 & \Gamma_{\mathbf{h}_n} & 0 \\ 0 & 0 & \Gamma_{\mathbf{h}_n} \end{pmatrix} \end{array}. \quad \text{(A3)}$$

APPENDIX B: CHANGE BETWEEN THE LOCAL COORDINATES AND FIXED COORDINATES

Using the polar angles, $\theta_{\mathbf{h}}$, $\phi_{\mathbf{h}}$ of the wave vector $\mathbf{k}_{\mathbf{h}}$, defined with respect to the fixed coordinate system $\{xyz\}$, The $\{xyz\}$ components are transformed to those of the local coordinates $\{123\}$ of a light of wave vectors $\mathbf{k}^{\pm}_{\mathbf{h}}$ by a 3×3 transformation matrix

$$\mathbf{R}^{\pm}_{\mathbf{h}}=\begin{pmatrix} R^{1x}_{\mathbf{h}} & R^{1y}_{\mathbf{h}} & R^{1z}_{\mathbf{h}} \\ R^{2x}_{\mathbf{h}} & R^{2y}_{\mathbf{h}} & R^{2z}_{\mathbf{h}} \\ R^{3x}_{\mathbf{h}} & R^{3y}_{\mathbf{h}} & R^{3z}_{\mathbf{h}} \end{pmatrix} =\begin{pmatrix} \cos\theta_{\mathbf{h}}\cos\varphi_{\mathbf{h}} & \cos\theta_{\mathbf{h}}\sin\varphi_{\mathbf{h}} & \mp\sin\theta_{\mathbf{h}} \\ \mp\sin\theta_{\mathbf{h}} & \cos\varphi_{\mathbf{h}} & 0 \\ \pm\sin\theta_{\mathbf{h}}\cos\varphi_{\mathbf{h}} & \pm\sin\theta_{\mathbf{h}}\sin\varphi_{\mathbf{h}} & \cos\theta_{\mathbf{h}} \end{pmatrix}. \quad \text{(B1)}$$

The rule for transforming the tensor $\mathbf{T}^{++}_{\mathbf{hh}'}$ from fixed to local coordinates is then

$$\mathbf{T}^{++}_{\mathbf{hh}'} \to \mathbf{R}^{+}_{\mathbf{h}}\mathbf{T}^{++}_{\mathbf{hh}'}(\mathbf{R}^{+}_{\mathbf{h}'})^{\mathrm{t}} = \begin{pmatrix} R^{1x}_{\mathbf{h}} & R^{1y}_{\mathbf{h}} & R^{1z}_{\mathbf{h}} \\ R^{2x}_{\mathbf{h}} & R^{2y}_{\mathbf{h}} & R^{2z}_{\mathbf{h}} \\ R^{3x}_{\mathbf{h}} & R^{3y}_{\mathbf{h}} & R^{3z}_{\mathbf{h}} \end{pmatrix} \times \begin{pmatrix} T^{++}_{xx} & T^{++}_{xy} & T^{++}_{xz} \\ T^{++}_{yx} & T^{++}_{yy} & T^{++}_{yz} \\ T^{++}_{zx} & T^{++}_{zy} & T^{++}_{zz} \end{pmatrix} \begin{pmatrix} R^{1x}_{\mathbf{h}'} & R^{2x}_{\mathbf{h}'} & R^{3x}_{\mathbf{h}'} \\ R^{1y}_{\mathbf{h}'} & R^{2y}_{\mathbf{h}'} & R^{3y}_{\mathbf{h}'} \\ R^{1z}_{\mathbf{h}'} & R^{2z}_{\mathbf{h}'} & R^{3z}_{\mathbf{h}'} \end{pmatrix}^{\mathrm{t}}. \quad \text{(B2)}$$

This procedure causes the matrix elements related to the local coordinate 3 (i.e., third row or third column of the right-hand side) to vanish naturally. In this way, we are left with a 2×2 matrix denoted $\hat{\mathbf{T}}^{++}_{\mathbf{hh}'}$. By arranging $\hat{\mathbf{T}}^{++}_{\mathbf{hh}'}$, etc., according to the channel labels, we may construct a $4N\times 4N$ S matrix. This is the S matrix $\mathbf{S}$ defined by Eq. (23).

When we impose the boundary condition at the boundary mirrors on the x and y components of the electric field of channel $\mathbf{h}$, we have to return from the local coordinates $\{123\}$ to the $\{xyz\}$ system. For the components 1 and 2 of the jth eigenvector $\mathbf{v}^{(j)}_{\mathbf{h}}$ introduced in Eqs. (24) and (26), this is accomplished by

$$\begin{pmatrix} (v^{(j)}_{\mathbf{h}})_x \\ (v^{(j)}_{\mathbf{h}})_y \end{pmatrix} = (\mathbf{r}^{+}_{\mathrm{h}})^{\mathrm{t}} \begin{pmatrix} (v^{(j)}_{\mathbf{h}})_1 \\ (v^{(j)}_{\mathbf{h}})_2 \end{pmatrix}, \quad \text{(B3)}$$

where the 2×2 transformation matrix $(\mathbf{r}^{+}_{\mathrm{h}})^{\mathrm{t}}$ is the 2×2 upper left block of

$$(\mathbf{R}_{\mathbf{h}}{}^{+})^{-1} = (\mathbf{R}_{\mathbf{h}}{}^{+})^{\mathrm{t}} = \begin{pmatrix} (x,1) & (x,2) & (x,3) \\ (y,1) & (y,2) & (y,3) \\ (z,1) & (z,2) & (z,3) \end{pmatrix}, \quad \text{(B4)}$$

where $\mathbf{R}^{+}_{\mathbf{h}}$ is defined by (B1) and $(x,3)$, for example, is the direction cosine between the x and 3 axes. The (x,y) component of $\mathbf{v}^{(j)}_{\mathbf{h}}$ is obtained compactly by

$$\begin{pmatrix} x \\ y \end{pmatrix} = \mathbf{r}^{+}_{\mathbf{h}} \begin{pmatrix} 1 \\ 2 \end{pmatrix}, \quad \text{(B5)}$$

namely, the product $\mathbf{r}^{+}_{\mathbf{h}}\mathbf{v}^{(j)}_{\mathbf{h}}$ gives the x and y components of $\mathbf{v}^{(j)}_{\mathbf{h}}$. This product notation is used in Eq. (34).

APPENDIX C: REDUCTION OF THE MATRIX M′ OF EQ. (42)

In Eq. (5), we note

$$\Gamma_{\mathbf{h}}(\omega + \mathrm{i}\epsilon') = \sqrt{[(\omega+\mathrm{i}\epsilon')/c]^2 - (\mathbf{k}_{\parallel}+\mathbf{h})^2} = \sqrt{(\omega/c)^2 - (\mathbf{k}_{\parallel}+\mathbf{h})^2} + \mathrm{i}\epsilon \equiv \Gamma_{\mathbf{h}} + \mathrm{i}\epsilon \quad \text{(C1)}$$

with an infinitesimal $\epsilon(\epsilon>0)$, and hence

$$e^{\mathrm{i}\Gamma_{\mathbf{h}}(\omega+\mathrm{i}\epsilon')L} = e^{\mathrm{i}\Gamma_{\mathbf{h}}L-\epsilon L}. \quad \text{(C2)}$$

Thus,

$$\tan\Gamma_{\mathbf{h}}(\omega+\mathrm{i}\epsilon')L = -i\frac{\exp(\mathrm{i}\Gamma_{\mathbf{h}}L-\epsilon L) - \exp(-\mathrm{i}\Gamma_{\mathbf{h}}L+\epsilon L)}{\exp(\mathrm{i}\Gamma_{\mathbf{h}}L-\epsilon L) + \exp(-\mathrm{i}\Gamma_{\mathbf{h}}L+\epsilon L)}. \quad \text{(C3)}$$

In the limit $L\to\infty$, we obtain

$$\tan\Gamma_{\mathbf{h}}(\omega+\mathrm{i}\epsilon')L \to i, \quad (L\to\infty). \quad \text{(C4)}$$

Therefore, the $\mathbf{h}$ dependence, in the $(\mathbf{h},j)$ matrix element

$$1 - \tan\Gamma_{\mathbf{h}}(\omega+\mathrm{i}\epsilon')L\,\tan\delta^{(j)} \quad \text{(C5)}$$

of the matrix $\mathbf{M}'$ disappears, and we obtain Eq. (44).

[1] K. M. Ho, C. T. Chan, and C. M. Soukoulis, Phys. Rev. Lett. **65**, 3152 (1990).
[2] T. Ochiai and K. Sakoda, Phys. Rev. B **63**, 125107 (2001).
[3] S. Fan and J. D. Joannopoulos, Phys. Rev. B **65**, 235112 (2002).
[4] See, e.g., P. Fulde, J. Keller, and G. Zwicknagl, *Solid State Physics*, edited by F. Seits, D. Turnbull, and H. Ehrenreich (Academic, New York, 1988), Vol. 41, p. 2; A. C. Hewson, *The Kondo Problem to Heavy Fermions* (Cambridge University Press, Cambridge, 1993).
[5] See, e.g., G. D. Mahan, *Many-Particle Physics*, 3rd ed. (Kluwer Academic/Plenum, New York, 2000), p. 195.
[6] K. Ohtaka and Y. Tanabe, J. Phys. Soc. Jpn. **65**, 2276 (1996).
[7] K. Sakoda, Opt. Express **4**, 167 (1999); K. Sakoda, K. Ohtaka, and T. Ueta, *ibid.* **4**, 481 (1999).
[8] F. J. Garcia de Abajo, Phys. Rev. Lett. **82**, 2776 (1999); Phys. Rev. E **61**, 5743 (2000).
[9] K. Ohtaka and S. Yamaguti, Opt. Spectrosc. **91**, 506 (2001); Opt. Quantum Electron. **34**, 235 (2002).
[10] S. Yamaguti, J. Inoue, O. Haeberlé, and K. Ohtaka, Phys. Rev. B **66**, 195202 (2002).
[11] K. Ohtaka, Y. Suda, S. Nagano, T. Ueta, A. Imada, T. Koda, J. S. Bae, K. Mizuno, S. Yano, and Y. Segawa, Phys. Rev. B **61**, 5267 (2000).
[12] P. Lloyd, Proc. Phys. Soc. London **86**, 825 (1965).
[13] J. R. Birch, J. D. Dromey, and J. Lesurf, Infrared Phys. **21**, 225 (1981).
[14] T. Kondo (unpublished).
[15] K. Ohtaka, Phys. Rev. B **19**, 5057 (1979).
[16] K. Ohtaka, J. Phys. C **13**, 667 (1980).
[17] N. Stefanou, V. Karathanos, and A. Modinos, J. Phys.: Condens. Matter **4**, 7389 (1992); A. Modinos, N. Stefanou, and V. Yannopapas, Opt. Express **8**, 197 (2001).
[18] T. Kondo, M. Hangyo, S. Yamaguchi, S. Yano, Y. Segawa, and K. Ohtaka, Phys. Rev. B **66**, 033111 (2002).
[19] S. Yano, Y. Segawa, J. S. Bae, K. Mizuno, K. Ohtaka, and S. Yamaguchi, Phys. Rev. B **63**, 153316 (2001); S. Yano, Y. Segawa, J. S. Bae, K. Mizuno, S. Yamaguchi, and K. Ohtaka, Phys. Rev. B **66**, 075119 (2002).

[20] R. W. Wood, Philos. Mag. **4**, 396 (1902); J. W. S. Rayleigh, *ibid.* **14**, 60 (1907).
[21] L. D. Landau and E. M. Lifshitz, *Quantum Mechanics*, 2nd ed. (Pergamon, London, 1965), p. 565.
[22] K. Ohtaka and M. Inoue, Phys. Rev. B **25**, 677 (1982); M. Inoue, K. Ohtaka, and S. Yanagawa, *ibid.* **25**, 689 (1982).
[23] M. Bayer, T. Gutbrod, J. P. Reithmaier, A. Forchel, T. L. Reinecke, P. A. Knipp, A. A. Dremin, and V. D. Kulakovskii, Phys. Rev. Lett. **81**, 2582 (1998).
[24] T. Mukaiyama, K. Takeda, H. Miyazaki, Y. Jimba, and M. Kuwata-Gonokami, Phys. Rev. Lett. **82**, 4623 (1999).
[25] K. Ohtaka, J. Lightwave Technol. **17**, 2161 (1999).
[26] E. Yablonovitch, Phys. Rev. Lett. **58**, 2059 (1987).
[27] S. John and T. Quang, Phys. Rev. A **50**, 1764 (1994); T. Quang, M. Woldeyohannes, S. John, and G. S. Agarwal, Phys. Rev. Lett. **79**, 5238 (1997).
[28] T. Suzuki and P. K. L. Yu, J. Opt. Soc. Am. B **12**, 570 (1995).
[29] Z. Y. Li, L. L. Lin, and Z. O. Zhang, Phys. Rev. Lett. **84**, 4341 (2000).
[30] V. Lousse and J. P. Vigneron, Phys. Rev. B **64**, 201104 (2001).
[31] K. Joulain, R. Carminati, J-P. Mulet, and J-J. Greffet, Phys. Rev. B **68**, 245405 (2003).